SM41H-2578

Cluster Observations of Non Time Continuous Magnetosonic Waves

Simon N. Walker[1], Michael A. Balikhin[1], Scott A. Boardsen[2,3], and David G. Sibeck[3]

[1]ACSE, University of Sheffield, Sheffield, UK, Godard Planetary and Heliophysics Institute, University of Maryland, Baltimore, Maryland, USA [3]NASA/GSFC, Greenbelt, Maryland, USA

ABSTRACT

Observations of magnetosonic waves in the inner magnetosphere have always shown that the waves are time continuous when viewed in a time-frequency spectrogram. Recently, examples of magnetosonic waves with modulated, rising tone elements have been reported. New observations from Cluster also show the existence of other, intermittent occurrences of magnetosonic waves. In this paper we investigate the properties of these wave emissions to determine the causes of these non-time continuous emissions. We report on a statistical study of the rate of frequency change for the rising tone emission features and show that they are modulated by fluctuations in the magnetic field. The more intermittent emissions appear to be controlled by the plasma density.

INTRODUCTION

Equatorial magnetosonic waves are common within a wide range of L-shells, typically 3 < L < 8, inside the terrestrial magnetosphere. Occurring in the frequency range between the proton gyrofrequency ω_{cp} and the lower hybrid frequency ω_{LH} they consist of a set of discrete, banded emissions at harmonics of the proton gyrofrequency (Gurnett, 1976; Santolík *et al.*, 2002). The wave normal angle, the angle between the wave *k*-vector and external magnetic field direction, $\theta_{Bk} \approx 89°$ implies that these waves are restricted in spatial extent to the region ±10 ° of the magnetic equator (Russell *et al.*, 1970; Olsen *et al.*, 1987; Němec *et al.*, 2005). Simultaneous observations of the wave and particle environments as well as theoretical studies indicate that these waves are most probably generated via an ion ring type distribution (e.g. Perraut et al., 1982; Boardsen et al., 1992; Meredith et al., 2008; Horne et al., 2000; Chen et al., 2010; Balikhin et al., 2015) with $\partial f / \partial v_{\perp} > 0$.

The role of magnetosonic waves in the evolution of the electron environment within the radiation belts was first discussed by Horne et al., (2007). These interactions, occurring through the Landau resonance when $\theta_{Bk}<90°$, are capable of accelerating electrons to high energies such that these particles may pose a threat to spacecraft whose orbits cross the radiation belts.

Almost all previous reports indicate that magnetosonic waves occur continuously throughout the period of their observation. There have been only a few exceptions to this. The first was the observations of the trapping of magnetosonic waves within the plasmapause (Ma et al., 2014). These authors demonstrated that magnetosonic waves generated locally inside the plasmapause boundary may propagate inward, eventually becoming trapped within a limited radial region of the outer plasmasphere by large scale density structures. Further evidence was also presented for the trapping by small scale structures. The second type of non-temporally continuous observations of magnetosonic waves are the recently identified observations of rising tone magnetosonic waves by Fu et al., (2014), Boardsen et al., (2014), and Němec *et al.*, (2015) based on observations from THEMIS, Van Allen Probes, and Cluster respectively. These observations show the occurrence of individual sets of emissions whose frequency rises with time at a sweep rate of 1Hzs^{-1} in a similar manner similar to that observed for chorus emissions and modulated with a repetition time of the order 2-3 minutes with the emission elements turning on and off.

DATA SETS

Data collected by the Cluster spacecraft (Escoubet et al., 1997)

- Orbit inclination 135°
- Science Burst mode 1 operations
- Fluxgate magnetometer (FGM) (Balogh et al., 1997) - sampling rate 67 Hz
- Spatio-Temporal Analysis of Field Fluctuations (STAFF) search coil magnetometer (Cornilleau-wehrlin et al., 1997) – sampling rate 450 Hz
- Electric Fields and Waves (EFW) (Gustafsson et al., 1997) – spacecraft potential measuments sampling rate 5 Hz

RISING TONE EMISSIONS

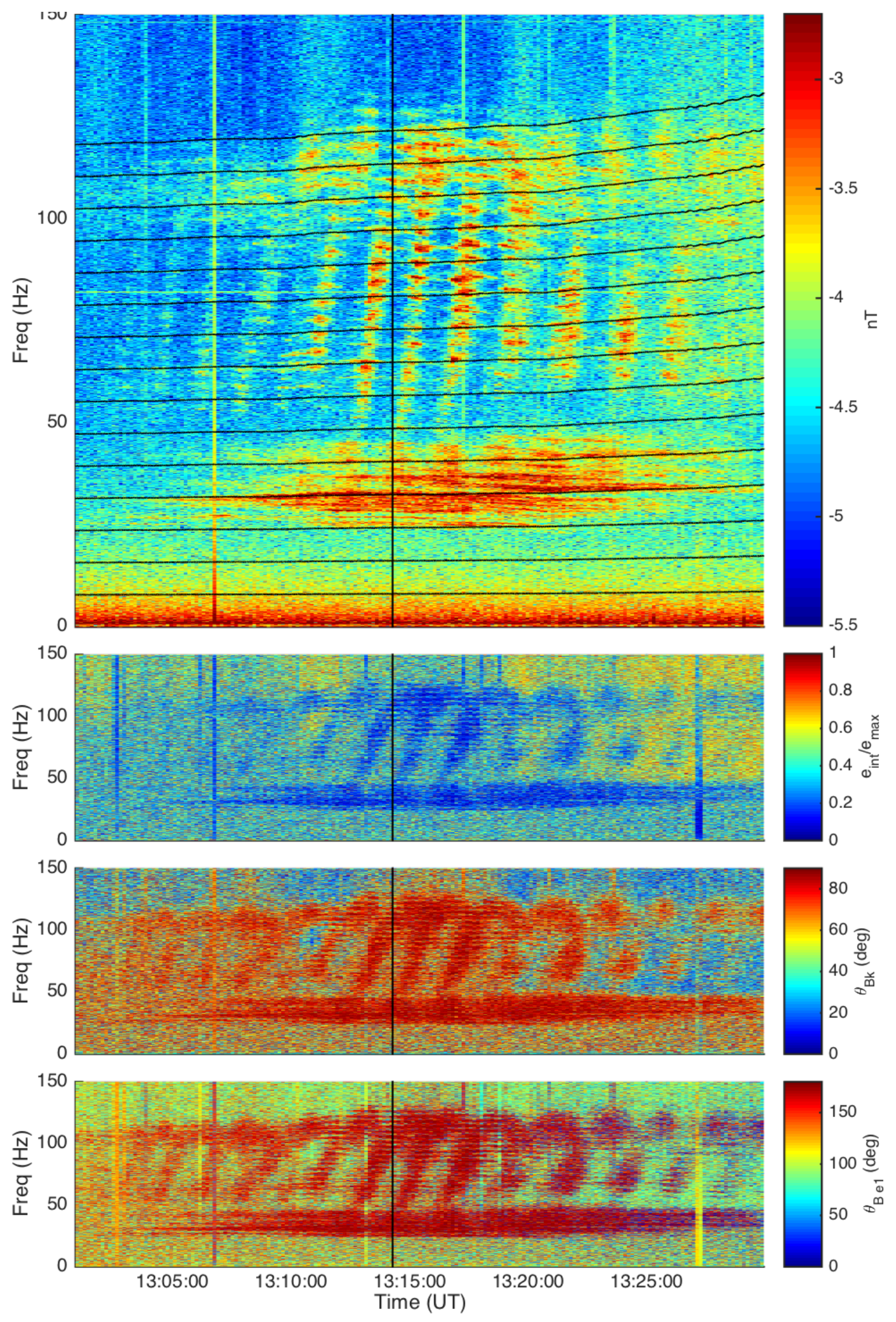

Spectral amplitudes of Bz (GSE) component

- black horizontal lines nΩ_p, n=[2:2:30]
- vertical black line indicates crossing of the magnetic equator

Ellipticity ($\lambda_{int}/\lambda_{max}$)
Waves are almost linearly polarised.

θ_{Bk}
Waves propagate perpendicular to the external magnetic field.

$\theta_{B\lambda max}$
Wave magnetic oscillations aligned with external field.

Figure 1. Rising tone emissions observed on 2005-08-18 by Cluster 2.

Figure 1 shows an example of the rising tone emissions observed by the Cluster STAFF search coil magnetometer on 2005-05-18. The wave properties clearly indicate that these are magnetosonic emissions since they are highly elliptically polarised, propagate almost perpendicular to the magnetic field and the magnetic vector of the oscillations is clearly aligned with the external magnetic field. It can also be seen that these parameters vary depending upon position relative to the magnetic equator. Compared to THEMIS and Van Allen Probe observations, Cluster typically only observes around 10 of these elements due to the nature of its highly inclined orbit.

To identify the sweep rate of these emissions the time of the maximum amplitude for each harmonic was determined for each emission element. Figure 2 shows how the time of the maximum amplitude varies with harmonic frequency for the 6 sets rising tone elements observed in the vicinity of the magnetic equator (which was crossed 13:14:16UT. For each element, a least squares fit was performed to determine the sweep rate. These values are shown in the legend box on the plot. In this example it is clearly seen that as Cluster 2 approaches the magnetic equator the gradient becomes steeper, changing from ~0.4Hzs^{-1} to ~0.9Hzs^{-1} in the vicinity of the equator before becoming less steep. Thus it appears that the sweep rate varies with distance from the magnetic equator.

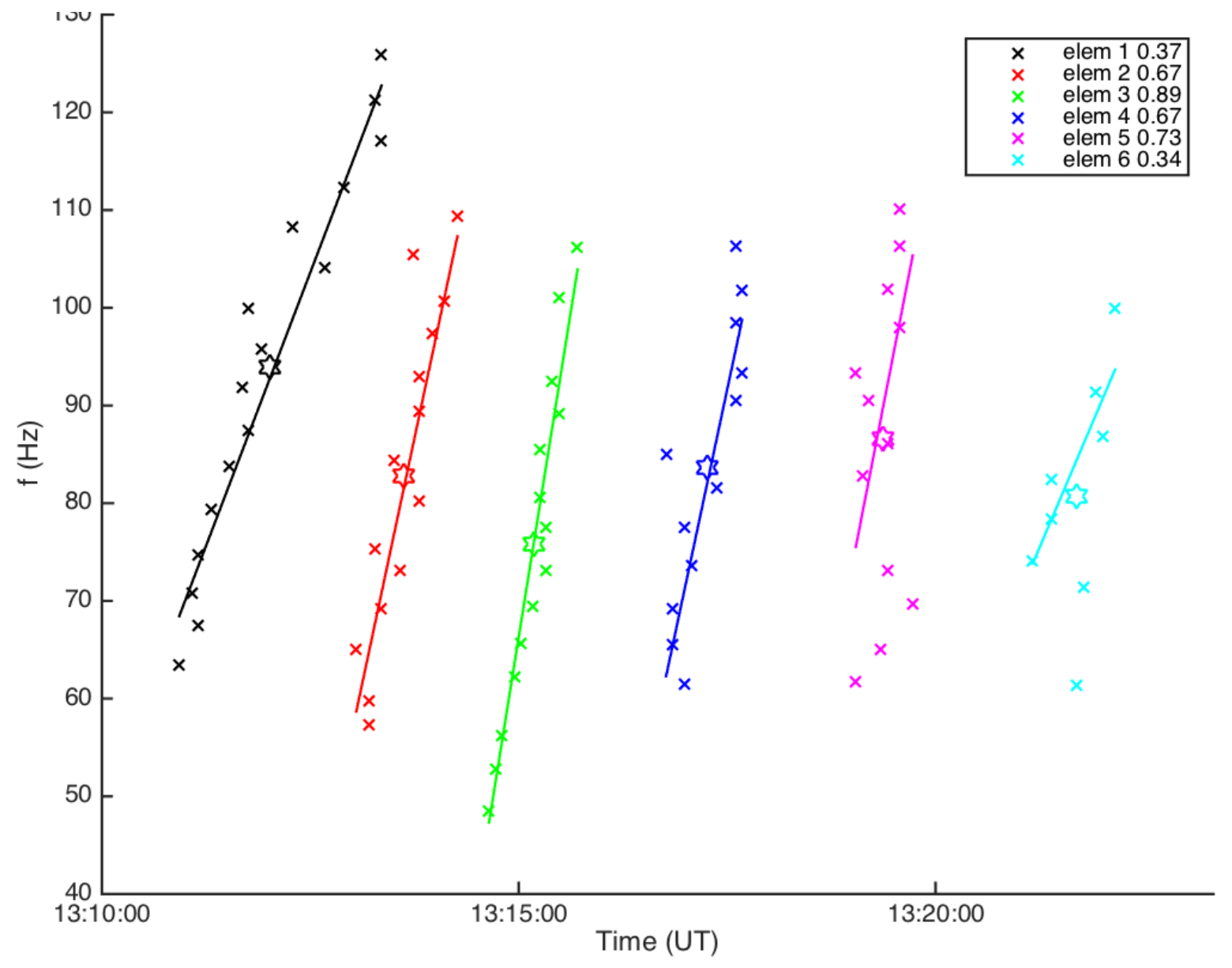

Figure 2. Frequency and time of the maximum wave amplitude.

TRAPPED EMISSIONS

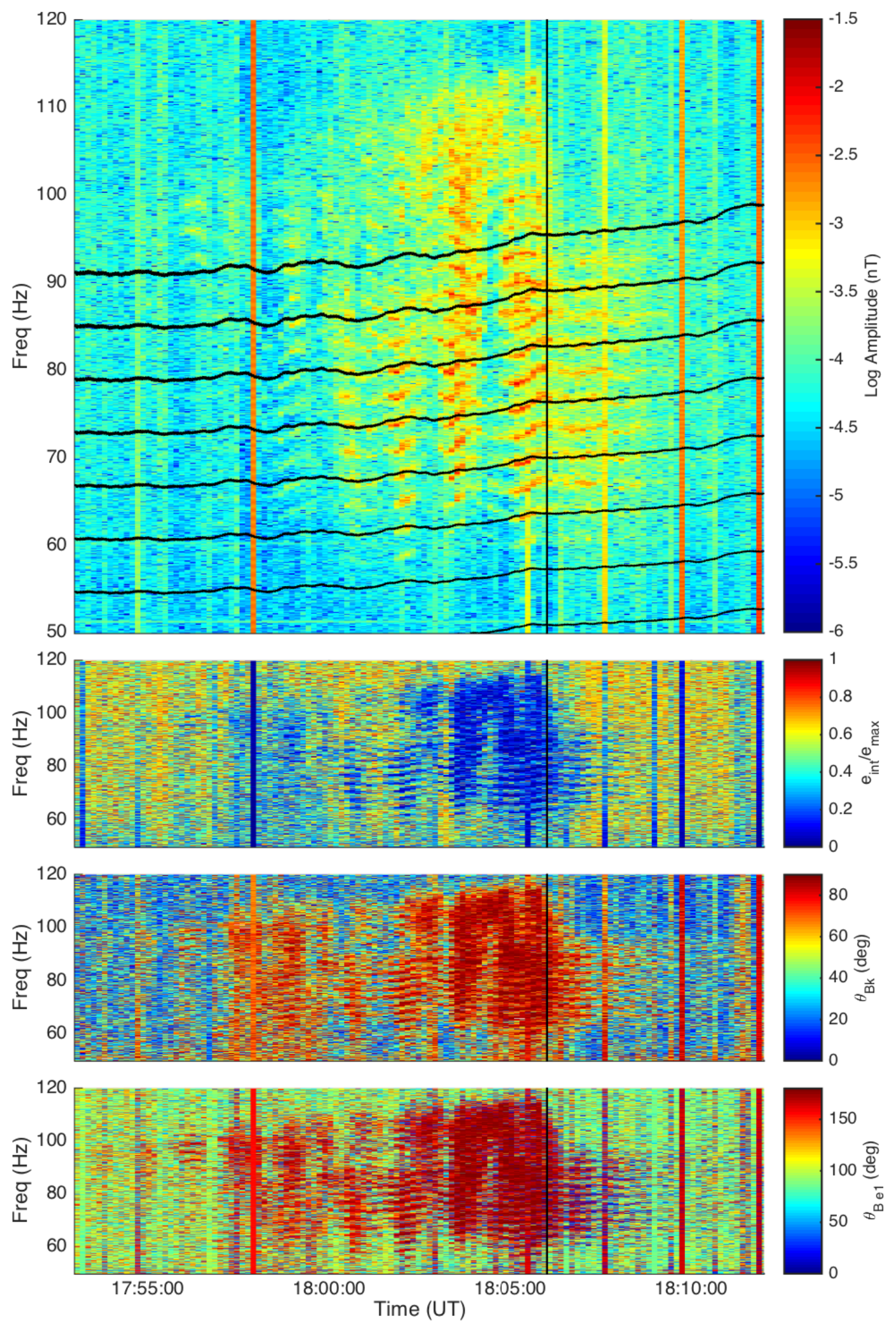

Spectral amplitudes of Bz (GSE) component

- black horizontal lines show the even proton gyroharmonics in the range 16-30Ω_p
- vertical black line indicates crossing of the magnetic equator

Ellipticity ($\lambda_{int}/\lambda_{max}$)
Waves are almost linearly polarised.

θ_{Bk}
Waves propagate perpendicular to the external magnetic field.

$\theta_{B\lambda max}$
Wave magnetic oscillations aligned with external field.

Figure 3. Magnetosonic waves emissions observed on 2005-09-13 by Cluster 1.

Figure 3 shows a second example of non-time continuous magnetosonic emissions observed on 2005-09-13 by Cluster 1 during a traversal of the geomagnetic equator, just outside the plasmapause boundary. In this case, the emissions do not exhibit the rising characteristics shown in Figure 1, the harmonic emissions for all elements tend to occur simultaneously.

There are broadly two types of harmonic emissions. Examples of the first type include the emissions observed around 17:59:02, 18:00:35 and 18:02:05 (frequencies below 90Hz), and emissions after 18:05:04. These waves are generated in-situ since their frequency follows changes observed in the local proton gyroharmonic frequencies. The second type, observed between 17:58 and 18:05 at frequencies above 80Hz consist of sets of emission lines whose frequencies either increase of decrease in time. For example, Table 1 shows the time of emissions and their sweep rate.

Table 1. Frequency sweep rates

Start time	End time	Sweep rate (Hzs^{-1})
17:58:37	17:59:29	0.048
18:00:54	18:01:54	-0.045
18:00:54	18:01:23	-0.089
18:01:26	18:02:03	0.082
18:02:00	18:02:27	-0.172

Since the frequency of these emissions is unrelated to the local proton gyrofrequency they must have propagated from their source region to the satellite location where they were observed.

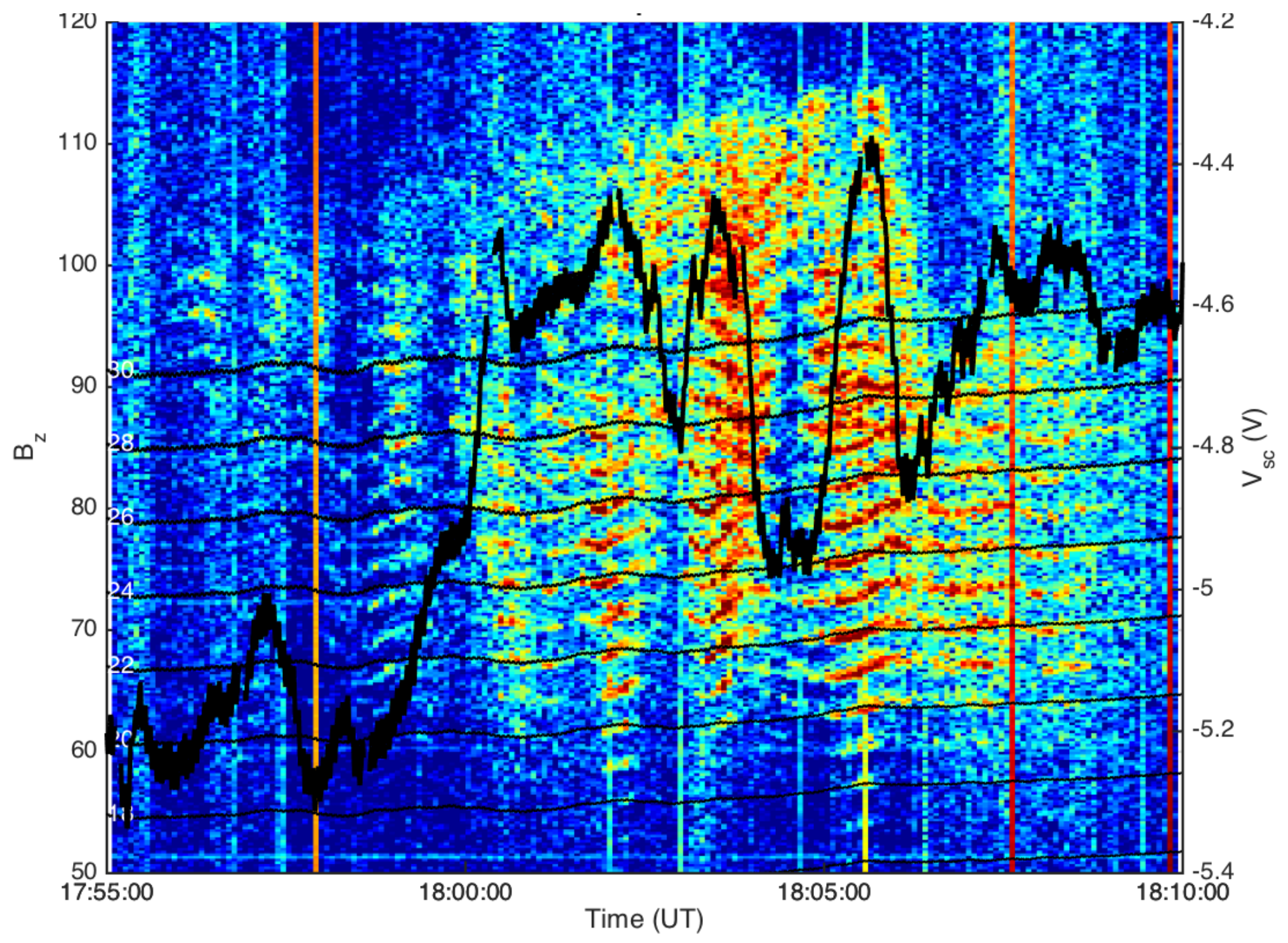

Figure 4. Relationship between wave emissions and electron density

Figure 4 shows the EFW spacecraft potential (black line), used as an proxy for measurements of the electron density. Increases in the electron density cause the spacecraft potential to become more positive. Enhancements in the wave emission amplitude are correlated with increases in the spacecraft potential and hence electron density.

CONCLUSIONS

Two examples of non time continuous have been shown.

The first is an example of periodic rising tone magnetosonic emissions, similar to those observed by THEMIS and Van Allen Probes.

- Individual harmonic emissions occur at harmonics of the local gyrofrequency, indicating local generation.
- The frequency sweep rate changes as the satellite approaches or recedes from the geomagnetic equator, being less steep at greater distances.

The second example shows non-periodic emissions.

- The occurrence of emissions at frequencies related to the local proton gyrofrequency appear to be correlated with increases in the spacecraft potential and hence electron density.
- These emissions are probably trapped within density ducts

Emissions are also observed whose frequency is unrelated to the local proton gyrofrequency.

- The emission bands have both positive and negative gradients.
- Generated in a remote source region
- Propagate to location of observation

ACKNOWLEDGEMENTS

This project has received funding from the *European Union's Horizon 2020 research and innovation programme* under grant agreement No 637302.

Balikhin, M. A. et al., (2015), Observations of discrete harmonics emerging from equatorial noise, Nat Commun, 6, doi: 10.1038/ncomms8703.

Balogh, A. et al., (1997), The Cluster magnetic field investigation, Sp. Sci. Rev., 79, 65–91, doi:10.1023/A:1004970907748.

Boardsen, S. A. et al., (1992), Funnel-shaped, low-frequency equatorial waves, J. Geophys. Res., 97, 14,967, doi:10.1029/92JA00827.

Boardsen, S. A. et al., (2014), Van allen probe observations of periodic rising frequencies of the fast magnetosonic mode, Geophys. Res. Lett., 41, 8161–8168, doi: 10.1002/2014GL062020.

Chen, L., et al. (2010), Global simulation of magnetosonic wave instability in the storm time magnetosphere, J. Geophys. Res. (Space Physics), 115(A11), A11222, doi:10.1029/2010JA015707.

Cornilleau-Wehrlin, N. et al., (1997), The Cluster Spatio-Temporal Analysis of Field Fluctuations (STAFF) experiment, Sp. Sci. Rev., 79, 107–136.

Escoubet, C. P. et al., (1997), Cluster - Science and mission overview, Sp. Sci. Rev., 79, 11–32.

Fu, H. S. et al., (2014), First observation of rising-tone magnetosonic waves, Geophys. Res. Lett., 41(21), 7419–7426, doi: 10.1002/2014GL061687.

Gurnett, D. A. (1976), Plasma wave interactions with energetic ions near the magnetic equator, J. Geophys. Res., 81, 2765–2770, doi: 10.1029/JA081i016p02765.

Horne, R. B. et al., (2000), Proton and electron heating by radially propagating fast magnetosonic waves, J. Geophys. Res., 105, 27,597–27,610, doi:10.1029/2000JA000018.

Ma, Q. et al., (2014), The trapping of equatorial magnetosonic waves in the earth's outer plasmasphere, Geophys. Res. Lett., 41, 6307– 6313, doi:10.1002/2014GL061414.

Nemec, F. et al., (2015), Equatorial noise emissions with quasiperiodic modulation of wave intensity, J. Geophys. Res. (Space Physics), 120, 2649–2661, doi:10.1002/2014JA020816.

Perraut, S. et al., (1982), A systematic study of ulf waves above fH+ from geos 1 and 2 measurements and their relationship with proton ring distributions, J. Geophys. Res. A, 87, 6219.

Russell, C. T. et al., (1970), OGO 3 observations of ELF noise in the magnetosphere: 2. the nature of the equatorial noise, J. Geophys. Res., 75, 755, doi:10.1029/JA075i004p00755.

Santolik, O. et al., (2002), Spatiotemporal variability and propagation of equatorial noise observed by Cluster, J. Geophys. Res. A, 107 (A12), 43–1, doi:10.1029/2001JA009159.